Synchrotron X-ray imaging of the formation of geometry deviations during percussion laser drilling with ultrashort pulses

Lukas Schneller[*1,2], Manuel Henn[1], Christoph Spurk[3], Marc Hummel[3,4], Alexander Olowinsky[4], Felix Beckmann[5], Julian Moosmann[5], Daniel Holder[1], Christian Hagenlocher[1], and Thomas Graf[1]

[1]*Institut für Strahlwerkzeuge IFSW, University Stuttgart, Pfaffenwaldring 43, 70569 Stuttgart Germany*
[2]*Graduate School of Excellence advanced Manufacturing Engineering (GSaME) Nobelstr. 12, 70569 Stuttgart Germany*
[3]*Chair for Laser Technology LLT, RWTH Aachen University, Steinbachstr. 15, 52074 Aachen, Germany*
[4]*Fraunhofer-Institute for Laser Technology ILT, Steinbachstr. 15, 52074 Aachen, Germany*
[5]*Institute of Materials Physics, Helmholtz-Zentrum Hereon, Max-Planck-Str. 1, 21502 Geesthacht, Germany*
* Corresponding author. E-mail address: lukas.schneller@ifsw.uni-stuttgart.de

The main objective of this work is to provide a basic understanding of the mechanisms and locations of defect formation during percussion laser drilling of microholes using ultrashort pulses. Through the application of high-speed synchrotron X-ray imaging, we have been able to observe the dynamic formation and evolution of these defects in real-time. Our findings indicate that the initial deviations in the borehole geometry are highly dependent on the applied laser fluence. Specifically, while higher peak fluences facilitate deeper drilling, there exists a critical threshold beyond which the position of these deviations begins to decrease as the fluence increases. This behavior can be partially predicted within a certain fluence range using an existing theoretical model, which our experimental observations have tested and validated. Consequently, this research not only advances our understanding of defect formation in laser drilling but also provides a predictive framework for optimizing drilling parameters to minimize defects and enhance borehole quality.

1. Introduction

The analysis of microholes in stainless steel, with respect to lateral extensions such as bulges and side channels, contingent on the polarization of the laser beam, has been limited to destructive analysis methods such as cross-sectional analysis or inlet/outlet images, which do not include the entire hole nor the temporal evolution of the borehole generation [1,2]. This paper presents the use of synchrotron X-ray imaging to quantitatively capture the deviations of the borehole at different depths during laser percussion drilling.

Förster's deep drilling model for high-quality percussion drilling, initially introduced in [1] and refined in [2] predicts the maximum depth limit

$$s_{\max} \approx d_f \cdot \sqrt{\frac{\left(\frac{H_0 - H_{\mathrm{th}}}{A}\right)^2 - H_{\mathrm{th}}^2 \cdot \left(\ln\left(\frac{H_0}{H_{\mathrm{th}}}\right)\right)^2}{8 \cdot H_{\mathrm{th}}^2 \cdot \ln\left(\frac{H_0}{H_{\mathrm{th}}}\right)}} \quad (1)$$

of percussion-drilled holes is dependent of the focal diameter of the laser d_f, the peak fluence H_0 and the ablation threshold fluence $H_{\mathrm{th}} = H_{\mathrm{A,th}}/A$, which is derived from the absorbed ablation threshold fluence $H_{\mathrm{A,th}}$ and the absorptivity A. It assumes a diffuse distribution of the radiation inside

a cone-shaped bore hole where the ablation at the tip takes place, when the absorbed irradiation $A \cdot H_{\mathrm{tip}}$ exceeds $H_{\mathrm{A,th}}$ so when $A \cdot H_{\mathrm{tip}} > H_{\mathrm{th}} \cdot A = H_{\mathrm{A,th}}$. In other words: Drilling stops when the absorbed fluence drops below the ablation threshold due to the increase in surface area within the borehole. Förster's model assumes that drilling takes place in phase 1 of the classical drilling model [3] and heat accumulation and plasma effects are avoided by selecting appropriate parameters like a relatively low repetition rate of f_{rep}=5 kHz. Based on the model the temporal evolution of the drilling depth already has been modeled [4]. In addition, a model was developed which shows the influence of the fluence at the exit of a borehole on the edge quality [5].

Based on Förster's suggestion that his model "describes a quality limit of laser drilling" [1], this paper examines whether a similar relationship can be recognized for the depth of the deviations that occur when using parameters that do not avoid heat accumulation and melt. If this depth is reached, defects occur, which are linked to a decrease in absorbed fluence below a specific threshold during the process, resulting in an increased melt formation and subsequent bad quality. [6–10]

2. Setup

Fig. 1 shows the imaging setup consisting of a X-ray beam of the synchrotron radiation source DESY (Deutsches Elektronen Synchrotron) with a diameter of approximately 2 mm, which results in a maximal measurable depth of $z_{meas,max} \approx 2$ mm. The X-rays radiate through the sample and are absorbed more the thicker the sample is. A scintillator converts the X-rays into visible radiation, which is recorded by a High-speed camera (i-SPEED 727, iX Cameras) at a framerate of 1 kHz and a spatial resolution of 856 px/mm. At the same time, a laser percussion process drills holes into the sample. This leads to an increased transmission at this point, which results in larger gray values.
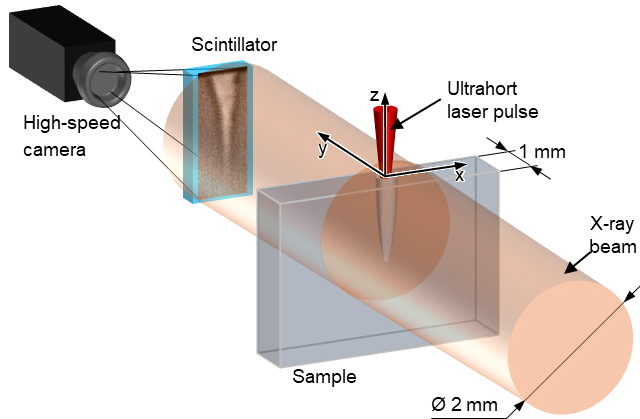

Fig. 1 X-ray Imaging setup. Modified from [11].

The experiments were performed with an ultrafast laser Carbide CB3 80 in 1 mm think stainless steel samples (St 1.4301 or AISI 304). A pulse duration τ of 1 ps was used. The drilling time was t=10 s, at a repetition rate of f_{rep}=50 kHz. Polarization was circular. The focus was positioned on the surface where the focal diameter was d_w=50 μm. Pulse energies E_P ranging from 50 μJ to 400 μJ resulted in peak fluences H_0 of 5.1 J/cm² to 40.7 J/cm². Smaller fluences were not used, as the drilling geometries become too small to be recognized with the existing setup.

3. Results and discussion

Fig. 2 shows a X-ray image sequence of a borehole drilled with a peak fluence of H_0 =15.3 J/cm². A typical depth progression can be observed, where the drilling speed is initially high and then gradually decreases, as described in the literature [12,13]. Table 1 shows the total depth and the average drilling speed for different drilling periods of the borehole shown in Fig. 2.

Table 1 Total depth and average drilling speed for different drilling periods.

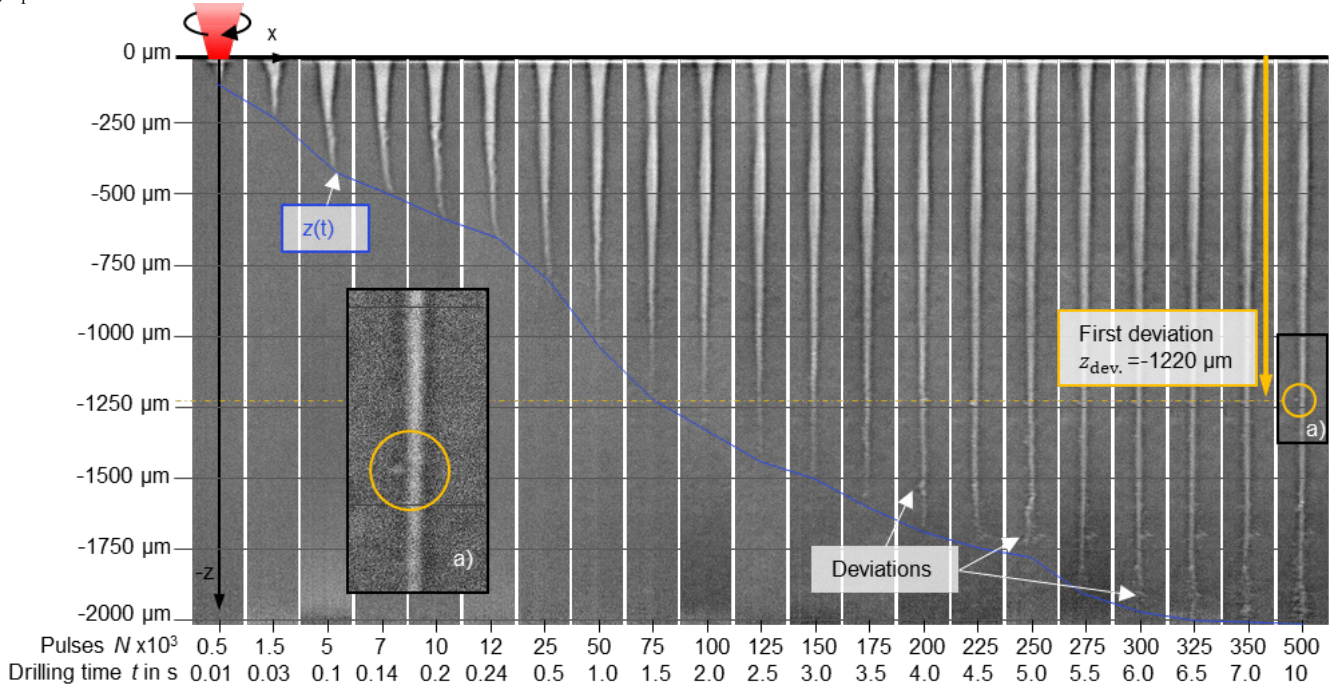| Drilling period Δt	No. of pulses N	Total depth $z(t)$	Average drilling speed v
in s	$\times 10^3$	in μm	in μm/s
0 - 0.5	0 … 25	790	1581
0.5 - 1	25 … 50	1030	480
1 - 2	50 … 100	1311	281
2 - 3	100 … 150	1499	188
3 - 4	150 … 200	1675	176
4 - 5	200 … 250	1758	83
5 - 6	250 … 300	1966	208
6 - 7	300 … 350	2011	45
7 - 10	350 … 500	2011	0

Fig. 2 Drilling progress of a borehole drilled with a peak fluence H_0 =15.3 J/cm². Note the non-linear X-axis. Inset a): The deviation closest to the surface that is visible after a drilling time of t=10 s occurs at z_{dev} = -1220 μm.

The average drilling speed decreases continuously, with one exception during 5 s<t<6 s, when the speed increases briefly. This is a typical behavior for phase 2 in the common drilling models. After approximately t=7 s the maximum drilling depth z_{max} was reached. A subsequent μ-CT examination of the borehole confirmed that there was no further depth progress after t=7 s, which corresponds to phase 3 in the common drilling models. After N=25,000 pulses bulging occurs between -250 μm > z > -750 μm as already described in [14]. In Fig. 2, deviations can be seen from a certain position z_{dev}. Deviations are defects next to the main borehole. With increasing depth, the deviations become more frequent and larger, sometimes in the form of side channels. The position of the first deviation can be read as a quality depth. Above this value a reasonable good quality is achieved. Below z_{dev} between z_{max} $z < z_{dev}$ a drilling progress still takes place, but deviations appear.

Fig. 3 shows X-ray images of boreholes drilled with different fluences H_0. The position of the first permanent deviation z_{dev} is marked with orange circles. Some of the deviations shown appear as voids that are no longer connected to the borehole, although they were initially connected during the formation process. At higher fluences the borehole diameter gets significantly wider and wavy structures occur probably because of an increased melt formation.
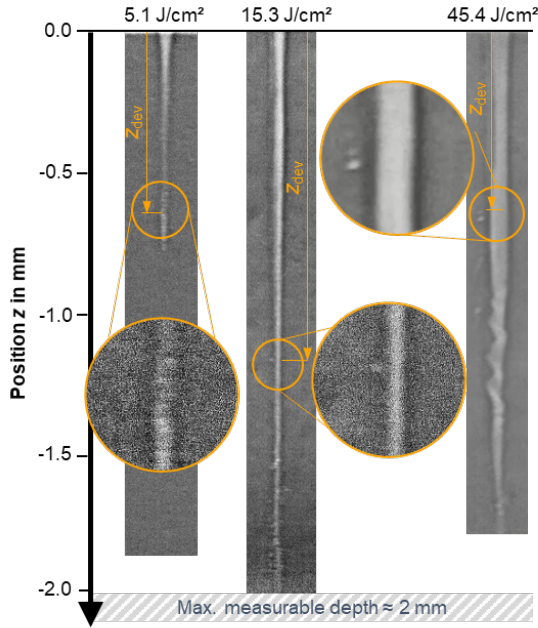

Fig. 3 Position of the first deviation z_{dev} (orange) visible in X-ray images of boreholes drilled with different fluences H_0. At high fluences the borehole diameter gets significantly wider and wavy structures occur.

This leads to a decrease of z_{dev} for higher fluences as also shown in Fig. 4 which shows the max. depth z_{max} of each borehole (blue) and the position of the first deviation (orange) over the peak fluence H_0. The black line is the theoretical depth limit s_{max} after Eq. (1) assuming an absorbed ablation threshold fluence $H_{A,th}$=0.106 J/cm^2 [1,15] and an absorptivity A=0.38. Until $H_0 \leq$15.2 J/cm^2 the position of the first deviation $z_{qual.}$ (orange) increases with the fluence. For higher fluences H_0>15.2 J/cm^2, the quality depth z_{dev} decreases with increasing fluence due to increased melt formation, which is visible as wave movements. Higher

fluences can also result in the generation of plasma inside the borehole [16–18], which "can act as a secondary drilling source" [18]. Additionally, the interaction of ablated particles with subsequent laser pulses becomes significant. Particle deposition inside the hole capillary can deflect the laser beam on the sidewalls, causing the observed deviations [18]. These combined effects - melt formation, plasma generation, particle interaction, and beam deflection can lead to more deviations occurring closer to the inlet.

Förster's model is intended for relatively small repetition rates that prevent "excessive influence of melt" [1]. In contrast, our experimental setup employs higher repetition rate and a small sample size in the Y-direction, conditions under which significant melt formation and heat accumulation can occur. These factors introduce complexities that Förster's model does not account for, leading to deviations between the model's predictions and our experimental observations in the max. borehole depth z_{max} (Fig. 4 blue).
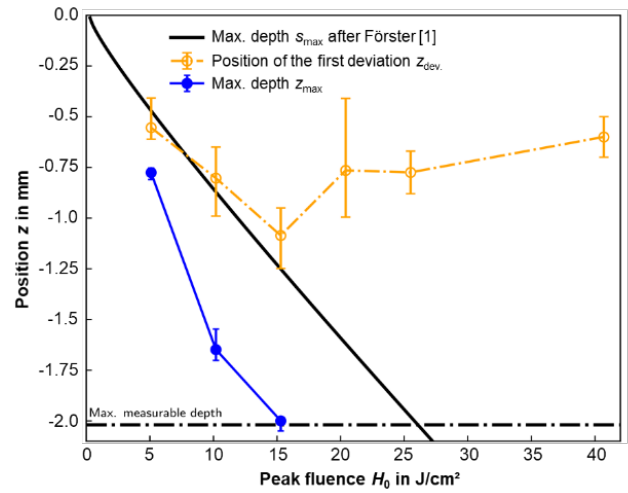

Fig. 4 Total depth (blue) and position of the first deviation z_{dev} (orange) over the peak fluence H_0. Error bars are min/max values of n=3 experiments. The black line is the max. depth s_{max} after Förster [1,2] given by Eq. (1) calculated with an absorptivity A=0.38 and an absorbed ablation threshold fluence $H_{A,th}$=0.106. The focal diameter was d_f = 50 μm. Blue: max. depth $z_{max.}$ of the borehole.

4. Conclusion

The study shows that the formation of deviations in microholes, as observed using an X-ray imaging technique, is highly dependent on the laser fluence applied during the drilling process. For fluences below 15 J/cm^2, the depth at which the first deviation occurs increases with fluence. At higher fluences, the drilling process shifts to a regime where various combined effects contribute to a change in defect formation mechanisms. Increased complexity and instability within the borehole lead to a significant melt formation and wavelike structures, causing the first deviation to occur at positions closer to the inlet. These findings underscore the importance of carefully controlling laser parameters to achieve high-quality microholes and provide a basis for further refinement of theoretical models to better predict and mitigate defect formation in high-fluence laser drilling processes.

References
[1] D.J. Förster, R. Weber, D. Holder, and T. Graf: Opt. Express, 26, (2018) 11546.
[2] H. Hügel, and T. Graf: "Materialbearbeitung mit Laser. Grundlagen und Verfahren", (Springer Vieweg, 2022) p.408.
[3] S. Döring, S. Richter, A. Tünnermann, and S. Nolte: Appl. Phys. A, 105, (2011) 69.
[4] D. Holder, R. Weber, T. Graf, V. Onuseit, D. Brinkmeier, D.J. Förster, and A. Feuer: Appl. Phys. A, 127, (2021) 301.
[5] A. Feuer, R. Weber, R. Feuer, D. Brinkmeier, and T. Graf: Appl. Phys. A, 127, (2021) 665.
[6] T.V. Kononenko, C. Freitag, D.N. Sovyk, A.B. Lukhter, K.V. Skvortsov, and V.I. Konov: Opt. Lasers Eng., 103, (2018) 65.
[7] A. Ancona, F. Röser, K. Rademaker, J. Limpert, S. Nolte, and A. Tünnermann: Opt. Express, 16, (2008) 8958.
[8] A. Feuer, D.J. Förster, R. Weber, and T. Graf. Lasers in Manufacturing Conference 2019, (2019) 1.
[9] R. Weber, T. Graf, P. Berger, V. Onuseit, M. Wiedenmann, C. Freitag, and A. Feuer: Opt. Express, 22, (2014) 11312.
[10] A. Feuer, C. Kunz, M. Kraus, V. Onuseit, R. Weber, T. Graf, D. Ingildeev, and F. Hermanutz. Proc. SPIE, Vol 6967, (2014), 89670H-6.
[11] L. Schneller, M. Henn, and M. Buser: "Setup for High-Speed Synchrotron X-Ray Imaging of Laser Drilling at the DESY", (DaRUS, 2024) p.1.
[12] S. Döring: "Analysis of the Hole Shape Evolution in Ultrashort Pulse Laser Drilling", (Cuvillier Verlag, 2014) p.54.
[13] T.V. Kononenko and V.I. Konov: Laser Phys., 11, (2001) 343.
[14] M. Henn, L. Schneller, D. Holder, D. Haasler, M. Hummel, F. Beckmann, J. Moosmann, C. Hagenlocher, and T. Graf. Proc. SPIE, Vol. 12873, (2024), 1287309-3.
[15] D. Brinkmeier, D. Holder, A. Loescher, C. Röcker, D.J. Förster, V. Onuseit, R. Weber, M. Abdou Ahmed, and T. Graf: Appl. Phys. A, 128, (2022) 35.
[16] Q. Li, L. Yang, C. Hou, O. Adeyemi, C. Chen, and Y. Wang: Optics and Lasers in Engineering, 114, (2019) 22.
[17] S.M. Klimentov, T.V. Kononenko, P.A. Pivovarov, S.V. Garnov, V.I. Konov, A.M. Prokhorov, D. Breitling, and F. Dausinger: Quantum Electron., 31, (2001) 378.
[18] S. Döring, T. Ullsperger, F. Heisler, S. Richter, A. Tünnermann, and S. Nolte: Phys. Procedia, 41, (2013) 431.